ARTICLE OPEN

Check for updates

Effect of thermo-oxidative aging on the Payne effect and hysteresis loss of carbon-black filled rubber vulcanizates

Boyuan Yin[1], Haibo Wen[1] and Wenbo Luo[2,3]✉

In the tire industry, the Payne effect and hysteresis loss of carbon-black (CB) filled rubber vulcanizates are the most concerning issues. CB filled rubber vulcanizates are susceptible to thermo-oxidative aging in the applications. In this paper, the effects of thermo-oxidative aging are investigated from experimental and theoretical aspects. The specimens are subjected to thermo-oxidative aging at 80, 100 and 120 °C for various periods of time ranging from 1 to 6 days and then the dynamic mechanical tests are conducted. The results show that both the storage modulus and the loss modulus increase with increasing aging time. The hysteresis loss of the material shows an increasing tendency with the increase of dynamic strain amplitude, aging time and aging temperature. The Kraus model is used to describe the Payne effect and a viscoelastic model consisting of dynamic strain amplitude and loss modulus is used to calculate the energy dissipation.

npj Materials Degradation (2022)6:94; https://doi.org/10.1038/s41529-022-00306-5

INTRODUCTION

The world's natural resources are non-renewable and only available to a limited extent. Nowadays, there is an increase in environmental awareness worldwide. This has consequences on market economies and the related product research and manufacturing[1]. It is well known that elastomers are of interest in many applications due to their tunable mechanical properties, as well as thermal and chemical stabilities[2].

Concerning the increasing interest in applying this material, intensive examinations are necessary. The increasing demand for high performance products with a simultaneous requirement for low price has stimulated the development of numerous efficient techniques. Natural rubber (NR) has been well recognized as one of the most important rubbers, and its properties are usually reinforced by the incorporation of CB to meet engineering demands[3]. However, the service conditions may bring about aging and degradation as a consequence of time-dependent and temperature-dependent mechanical properties, which can dramatically affect the service lifetime of rubbers. For the long-term properties of rubber-like materials, both the aging and dynamic properties are key factors in engineering applications. It is necessary to determine the thermal aging and mechanical properties of CB filled rubber products as this can help identify what applications the resulting rubbers are suitable for. Hence, reliable characterization techniques for the determination have to be provided. One of many well-established methods that enable accurate quantification of material thermo mechanical properties is dynamic mechanical analysis (DMA)[4,5]. Although many reports have focused on the aging mechanisms and mechanical performances of aged rubber products[6–9], only a few studies have been provided regarding the thermorheological properties, such as the storage modulus and the loss modulus, which are related to the phase angle (δ) on the basis of stress–strain behavior[10,11].

In addition, under cyclic loading, the CB filled rubber exhibits apparent viscoelastic nonlinearity (Payne effect) and hysteresis loss. Payne effect has been ascribed to the mechanisms, such as breakup/reformation of filler network or polymer-filler network, agglomeration/ deagglomeration of filler aggregates, chains desorption from nanoparticles, and disentanglement of adsorbed chains[12]. Payne effect is very important in the tire industry because dynamic nonlinearity is in the range of strain amplitudes most frequently encountered in reality[13]. For this reason, many works have been conducted to explain this phenomenon, mainly focusing on the frequency-, prestrain- and temperature-dependence[4,12]. Currently, an increasing number of researchers are investigating the Payne effect from the aspect of micro-structure evolution in a particular experimental situation by using SEM, NMR and AFM[14–16]. Meanwhile, in the process of Payne effect investigation, a series of constitutive models have been proposed to reproduce this kind of mechanical behavior of CB filled rubbers. These models can generally be classified into two groups: filler network structural models and matrix-filler interface bonding and bonding failure models[17]. Kraus was the first to develop a phenomenological constitutive model to interpret the Payne effect of rubber-like materials, which was based on filler network breakage, by supposing a dynamic equilibrium between the breakage and recovery of weak physical bonds under cyclic loading conditions[18,19]. Although the Kraus model has been widely used for the effect of thermo-oxidative aging on the Payne effect, there is not much research on this issue. With increasing aging time, a general consensus is that the crosslink density of rubber-like materials changes obviously, which results in a change in mechanical behavior[10,20]. Li[8] demonstrated that the crosslink density of the CB filled rubber vulcanizates aged at 100 and 120 °C, measured by equilibrium swelling method, increases with the increase of aging time. As for the Payne effect, it was reported that both storage and loss moduli increase with increasing aging time[21,22], which is mainly due to the increasing crosslink density during the aging process. Besides, it should be noticed that prolonged heating at/over 70 °C is apt to cause post-vulcanization[23], which generates more crosslinks[23,24]. However, it is recognized that there are two competitive mechanisms during aging: chain crosslinking and chain scission[25]. Hou[11] investigated

[1]School of Civil Engineering, Hunan University of Science and Technology, Xiangtan 411201, China. [2]School of Civil Engineering, Changsha University, Changsha 410022, China. [3]Hunan Key Laboratory of Geomechanics and Engineering Safety, Xiangtan University, Xiangtan 411105, China. ✉email: luowenbo@ccsu.edu.cn

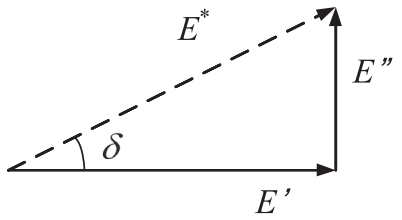

Fig. 1 Relationship among E', E'' and tan δ. The loss factor tan δ is defined as the ratio of the loss and storage modulus.

the influence of aging induced network variation on the Payne effect of isoprene rubber vulcanizates, and the results showed that the crosslink density increases first and then decreases with the increase of aging time, and the storage modulus also changes in the same trend, indicating that the crosslinking dominates in the early stage of aging. With proceeding of the aging, polysulfide, disulfide and monosulfide bonds densities change due to breaking and conversion, the bond breaking causes network defects including dangling and free chains, and results in the change of dynamic mechanical properties and hysteresis loss[26]. It is worth noting that the predominance of the two competitive mechanisms during aging is due to various factors, in particular to the composition of the material[25]. For example, Wang[27] measured the crosslinking density of three kinds of CB filled rubber materials (SIBR-CB, SSBR-CB, and Nd-IR-CB) during the aging process, and the results showed that crosslinking is the dominant reaction in SIBR-CB and SSBR-CB samples, while the Nd-IR-CB sample undergoes scission.

Moreover, the Payne effect reflects a way of hysteresis loss under cyclic loading and the hysteresis loss gradually translates into heat, which can affect the mechanical property on the one hand and can result in thermo-oxidative aging on the other hand. To understand the hysteresis loss mechanism, extensive research has been conducted using experimental investigation or constitutive characterization[28,29]. However, these works do not pay attention to the influence of thermo-oxidative aging on the hysteresis loss. Therefore, it is necessary to study the effects of thermo-oxidative aging on the Payne effect and hysteresis loss of the CB filled rubber-like materials.

To this end, this paper attempts to study the thermo-oxidative aging-dependence of the Payne effect and hysteresis loss of filled rubber. In the classic theory framework, the Kraus model is employed to model the aging time and temperature dependence of the Payne effect and the comparison is made in detail according to the prediction of hysteresis loss.

RESULTS AND DISCUSSION

Hysteresis loss

Dynamic mechanical analysis (DMA) is an indispensable and effective tool for determining the viscoelastic properties of polymers and polymer composite materials, such as crosslinking density[30], dynamic/complex viscosity and storage/loss compliance[31,32].The storage modulus E' or dynamic modulus is typically related to the Young's modulus and refers to the ability to store energy applied to it for future purposes. The loss modulus E'' is often considered as the tendency to dissipate energy[33]. The loss factor tan δ, as shown in Fig. 1, is defined as the ratio of the loss and storage modulus:

$$\tan\delta = E''/E' \tag{1}$$

Generally, the test specimen is loaded with a sinusoidal strain-controlled process, and the strain excitation $\varepsilon(t)$ can be expressed in the following form:

$$\varepsilon(t) = \varepsilon_0 + \Delta\varepsilon\sin(\omega t) \tag{2}$$

where ε_0 is the prestrain, $\Delta\varepsilon$ is the dynamic strain amplitude, and ω is the angular frequency. The corresponding stress response $\sigma(t)$ of the specimen can be defined as:

$$\sigma(t) = \sigma_0 + \Delta\sigma\sin(\omega t + \delta) \tag{3}$$

where σ_0 is the static stress, $\Delta\sigma$ is the stress amplitude, and δ is the phase angle between the applied strain and the resulting stress. The storage modulus E' and the loss modulus E'' are determined by standard methods:

$$E' = \frac{\Delta\sigma}{\Delta\varepsilon}\cos\delta \tag{4}$$

$$E'' = \frac{\Delta\sigma}{\Delta\varepsilon}\sin\delta \tag{5}$$

By substituting Eqs. (4) and (5) into Eq. (3), the dynamic stress response can also be rewritten as:

$$\sigma(t) = \sigma_0 + \Delta\varepsilon[E'\sin(\omega t) + E''\cos(\omega t)] \tag{6}$$

In addition, in the process of cyclic loading, the strain energy W over one period can be calculated by the following equation:

$$W = \int_0^{\frac{2\pi}{\omega}}\sigma d\varepsilon = \omega(\Delta\varepsilon)^2\int_0^{\frac{2\pi}{\omega}}\left[E'\sin(\omega t)\cos(\omega t) + E''\cos^2(\omega t)\right]dt \tag{7}$$

It is well known that in the process of cyclic loading, the energy consists of two parts: the stored energy and dissipated energy. The dissipated energy, named hysteresis loss, can be calculated by the area of the hysteresis loop, which makes the temperature rise of the deformed material. In addition, the dissipated energy is only related to the loss modulus, and it can be expressed in the following form:

$$D = W_{\text{loop}} = \pi(\Delta\varepsilon)^2 E'' \tag{8}$$

Kraus model

The Payne effect is a representative feature of the behavior of CB filled rubber materials. In other words, with increasing strain amplitude, the storage modulus decreases, and the loss modulus increases at first and then decreases. Kraus was the first to develop a phenomenological constitutive model to interpret the Payne effect of rubber-like materials, which was based on filler network breakage, by supposing a dynamic equilibrium between the breakage and recovery of weak physical bonds under cyclic loading conditions[17,18]. In the Kraus model, the storage modulus and the loss modulus have the following expressions[34]:

$$E'(\Delta\varepsilon) = E'_\infty + \frac{E'_0 - E'_\infty}{1 + (\Delta\varepsilon/\Delta\varepsilon_c)^{2m}} = E'_0 - \Delta E' + \frac{\Delta E'}{1 + (\Delta\varepsilon/\Delta\varepsilon_c)^{2m}} \tag{9}$$

$$E''(\Delta\varepsilon) = E''_\infty + \frac{2(E''_m - E''_\infty)(\Delta\varepsilon/\Delta\varepsilon_c)^m}{1 + (\Delta\varepsilon/\Delta\varepsilon_c)^{2m}} \tag{10}$$

where $\Delta\varepsilon_c$ is a characteristic value of the strain amplitude at which the loss modulus reaches the maximum value E''_m; E'_0 is the storage modulus when the dynamic strain amplitude is <0.01%; E'_∞ and E''_∞ are the asymptotic plateau values of the storage modulus and loss modulus at large strain amplitudes, respectively;E''_∞ usually tends to be 0 for rubber-like materials[29]; $\Delta E'\left(=E'_0 - E'_\infty\right)$is the excess storage modulus; and m is a nonnegative phenomenological exponent, which gives the strain sensitivity of the mechanism of filler-filler contact breakage and defines the shape of the storage modulus and loss modulus curves[29,34].

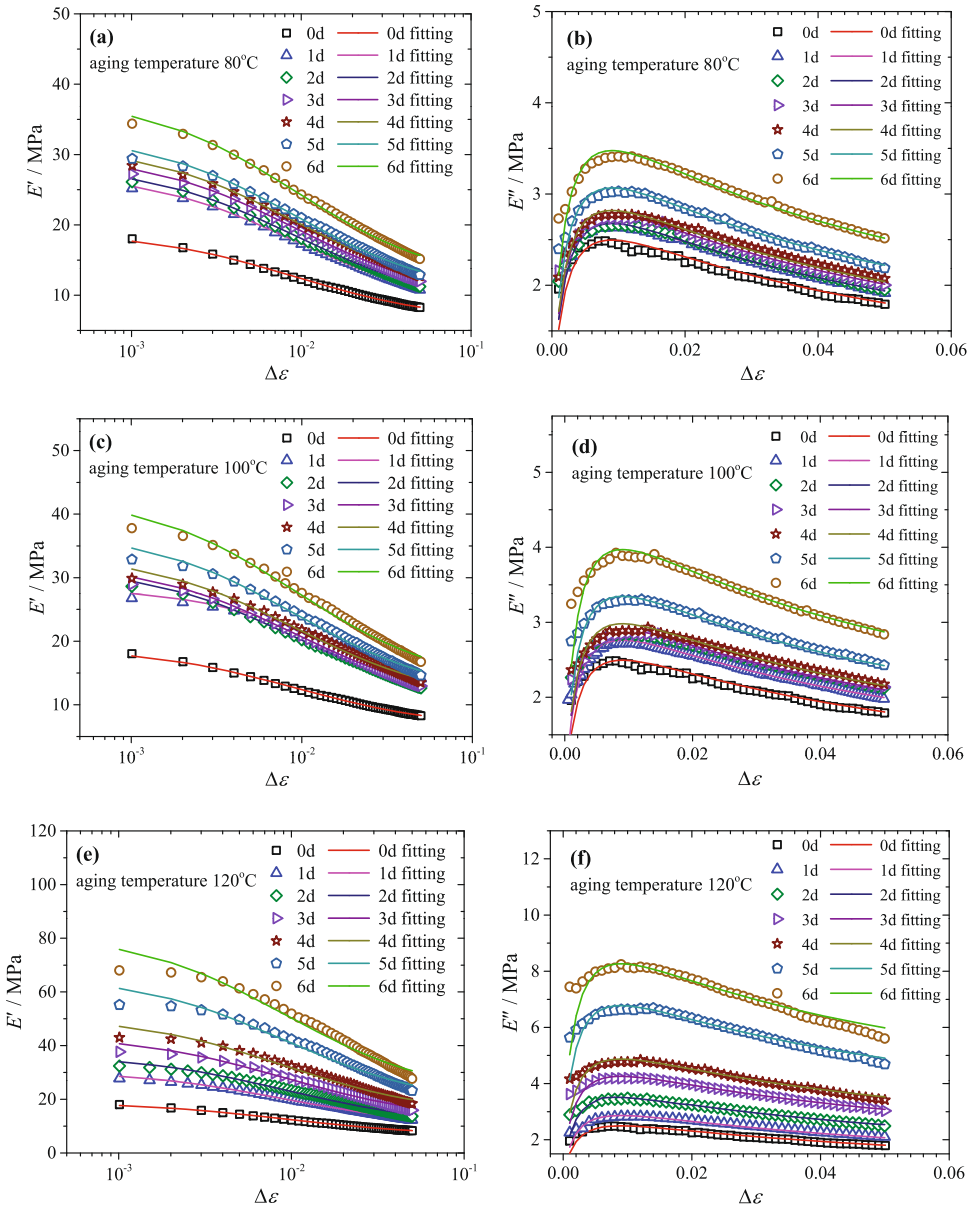

Fig. 2 Dynamic mechanical modulus vs. strain amplitude. Scatters are the experemental resutls for various aging times and temperatures, and solid lines are the modelling results. **a**, **b** The storage modulus and the loss modulus respectively for aging temperature 80 °C, **c**, **d** the storage modulus and the loss modulus respectively for aging temperature 100 °C, **e**, **f** the storage modulus and the loss modulus respectively for aging temperature 120 °C.

Evaluation of thermo-oxidative aging dependent Payne effect

Figure 2 shows the Payne effect of thermo-oxidative aging samples. In the test dynamic strain range, the storage modulus and loss modulus are shown as a function of the applied dynamic strain amplitude and thermo-oxidative aging time. The storage modulus decreases gradually with increasing strain amplitude and there is a typical loss peek for the loss modulus. It can be seen that in all cases both the storage modulus and loss moduli increase with increasing aging time, which is mainly due to the increase of crosslink density of the material during the aging process[22]. Besides, it should be noticed that prolonged heating above 70 °C is apt to cause post-vulcanization, which generates more cross-links[23]. According to the Kraus model, the material parameters in Eqs. (9) and (10) can be derived by fitting the experimental data. In the process of fitting, it should be noted that the parameter m is a constant value of 0.49. It has been reported that the exponent m is independent of frequency and temperature[29], which verifies the accuracy of the fitting results.

The Payne effect can be characterized by the difference ($\Delta E' = E'_0 - E'_\infty$) between the maximum value E'_0 and minimum value E'_∞ of the storage modulus in the dynamic strain amplitude range, as shown in Fig. 3. It is noted that for all aging temperatures studied, the Payne effect maintains the same trend, which means that the difference between the maximum value and the minimum value at the aging temperatures measured practically increases. Moreover, the Payne effect for aging temperature of 120 °C is more obvious when compared with those for aging temperatures of 80 and 100 °C.

$\Delta\varepsilon_c$ is a characteristic value of the strain amplitude at which the loss modulus reaches its maximum value E''_m. Figure 2 shows that $\Delta\varepsilon_c$ is a constant value of 0.9%. According to the Kraus model, the material parameter E''_m is shown in Fig. 4. For all aging temperatures, when the aging time reaches 4 days, E''_m increases

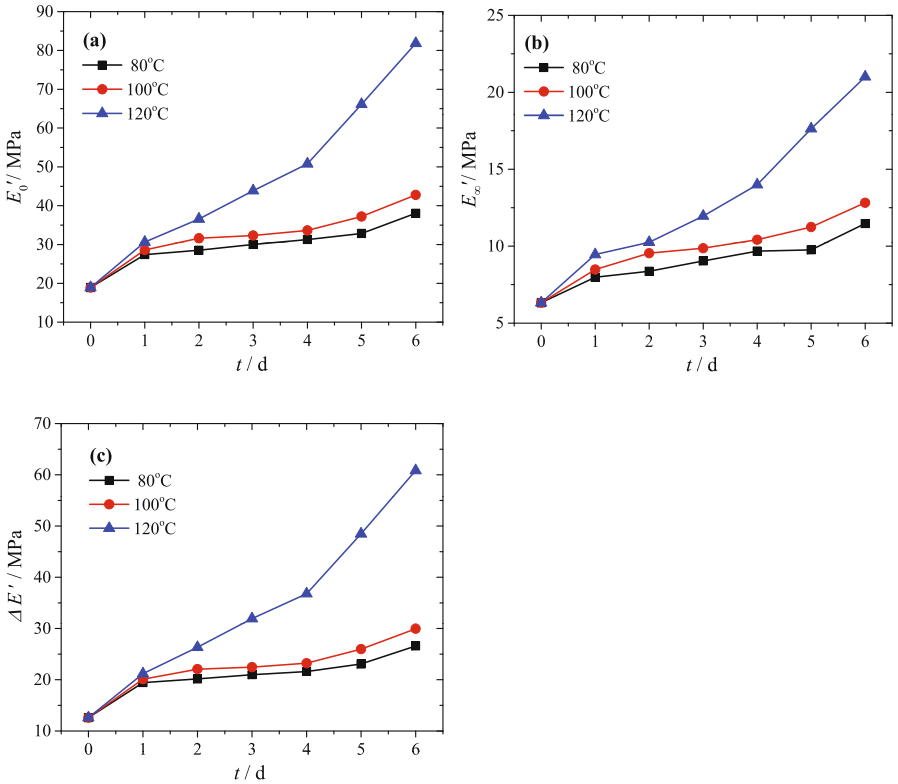

Fig. 3 Changes of Kraus model parameters. a The tendency of the parameter E_0' with the aging time for various aging temperatures, **b** the tendency of the parameter E_∞' with the aging time for various aging temperatures and **c** the tendency of the parameter $\Delta E_0'$ with the aging time for various aging temperatures.

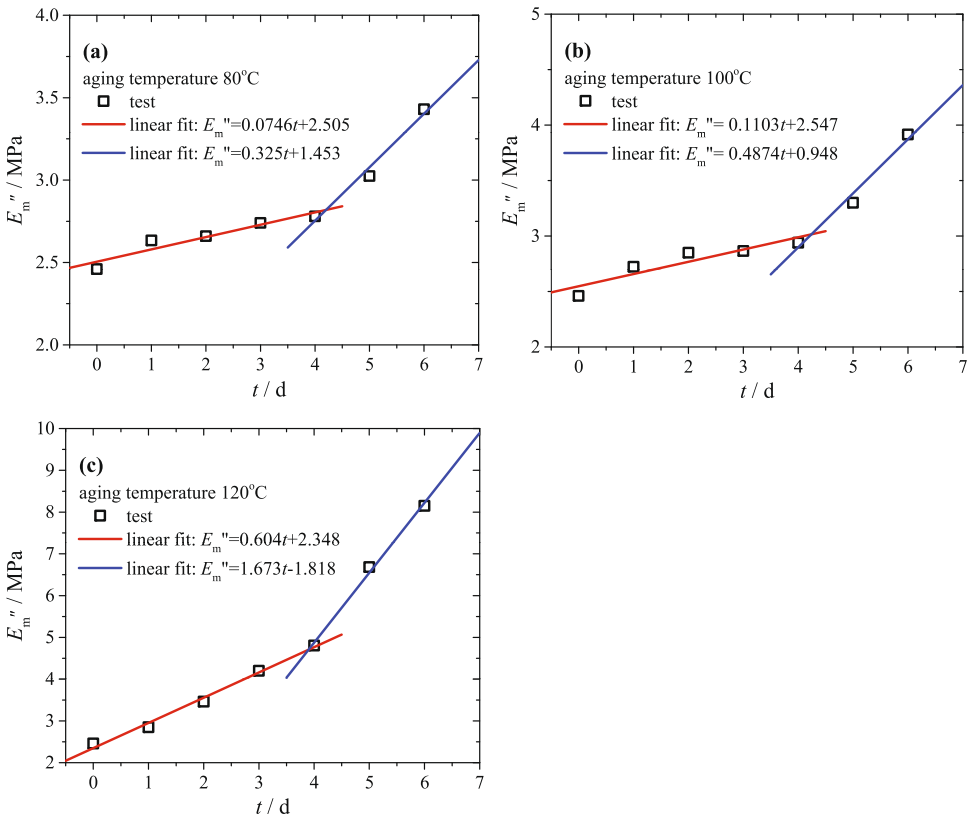

Fig. 4 Variation of parameter E_m'' with aging time. Scatters are parameter E_m'', and solid lines are linear fit results. **a** The results for aging temperature 80 °C, **b** the results for aging temperature 100 °C, **c** the results for aging temperature 120 °C.

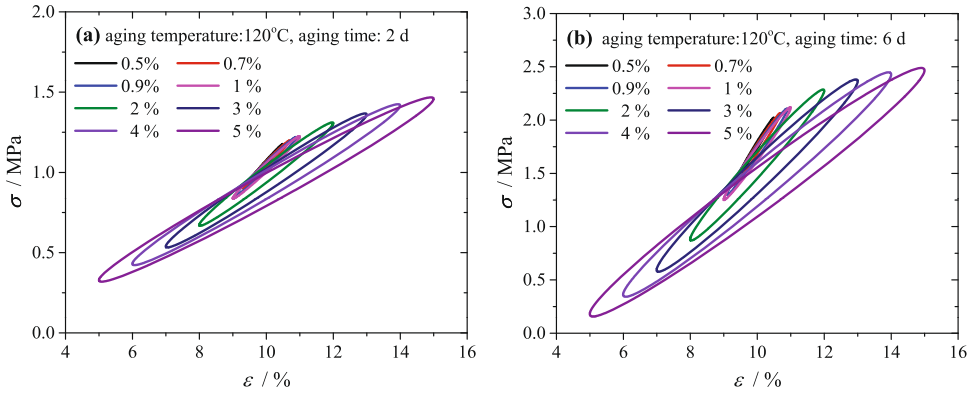

Fig. 5 Steady-state hysteresis loops. The hysteresis loops of the material aged at 120 ℃ for different periods of time: **a** 2 days and **b** 6 days. The curves are obtained under various dynamic strain amplitudes, i.e. 0.5%, 0.7%, 0.9%, 1%, 2%, 3%, 4% and 5%.

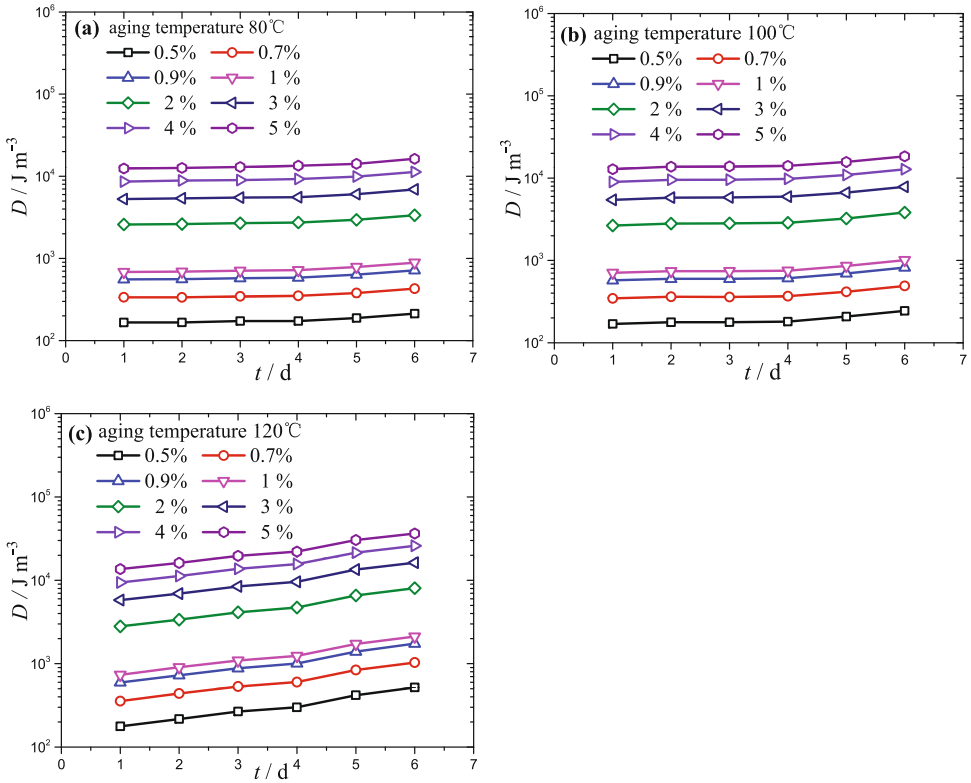

Fig. 6 Hysteresis loss as a function of aging time. The symbols represent the hysteresis loss under various dynamic strain amplitudes, i.e. 0.5%, 0.7%, 0.9%, 1%, 2%, 3%, 4% and 5%. The hysteresis loss increases with the aging time and dynamic strain amplitude for various aging temperatures: **a** 80 ℃ , **b** 100 ℃ and **c** 120 ℃.

dramatically. This indicates that an aging time of 4 days can be regarded as the knee point for the studied material, at which the change rate with respect to aging time of the parameters in loss modulus dramatically changes. In addition, it is obvious that there are nearly two linear phases in the tested aging time range for each aging temperature, and the linear fitting results of E''_m are shown in Fig. 4. Therefore, the loss modulus of the tested CB filled rubber can be quantitatively expressed as a function of dynamic strain amplitude and aging time by the following equation:

$$E''(\Delta\varepsilon) = \frac{2E''_m(\Delta\varepsilon/0.009)^{0.49}}{1+(\Delta\varepsilon/0.009)^{0.98}} \tag{11}$$

where E''_m is a function of aging time, and the expressions of E''_m are shown in Fig. 4. Below, the hysteresis loss on the basis of loss modulus has been discussed by substituting Eq. (11) into Eq. (8).

Prediction of hysteresis loss

Under cycle loading in the process of the dynamic amplitude sweep test, the CB filled natural rubber exhibits hysteresis loss properties because of the out-of-phase stress and strain. The hysteresis loops obtained from the dynamic amplitude sweep test are presented in Fig. 5. Since there are many hysteresis loops and there is no need to show all loops, so the following hysteresis loops are chosen as examples under the conditions of aging times of 2 days and 6 days, aging temperature of 120 °C, and various dynamic strain amplitudes, i.e., 0.5%, 0.7%, 0.9%, 1%, 2%, 3%, 4% and 5%. In addition, the hysteresis losses of other aging and loading conditions are exhibited in Fig. 6. The results show that the slope of the secant to the hysteresis loop decreases gradually with increasing dynamic strain amplitude, which represents the characteristic of the dynamic stiffness of the material. The slope change trend of the hysteresis loop is consistent with the dynamic

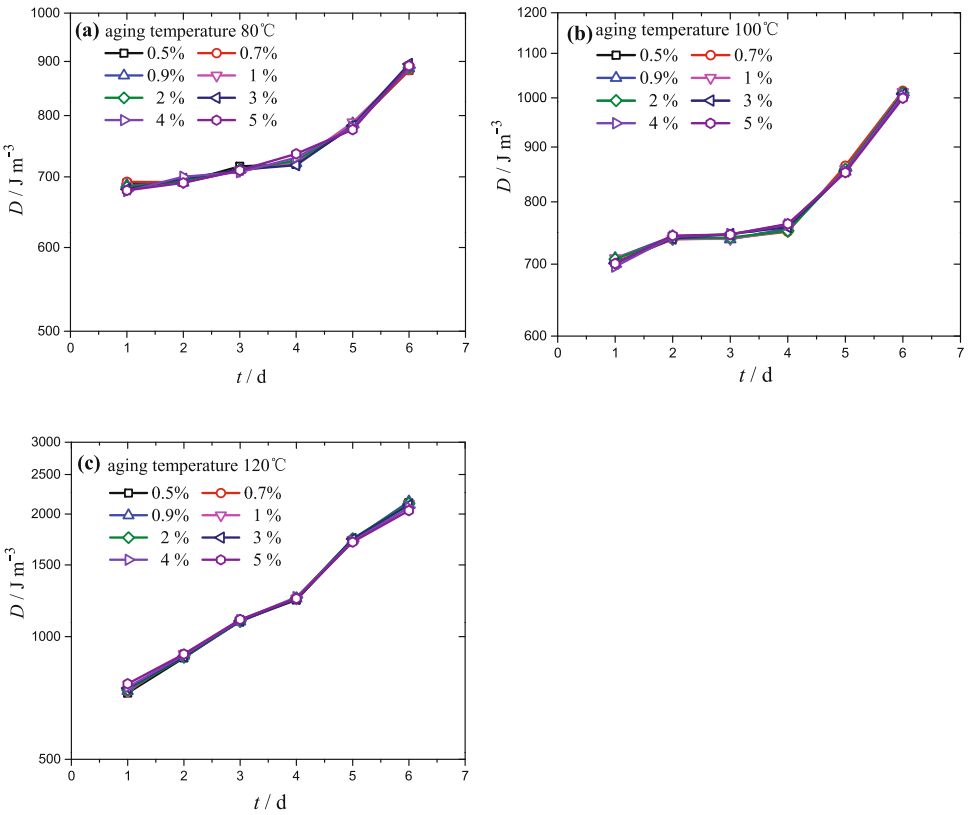

Fig. 7 Master curve of hysteresis loss. The master curve at a reference dynamic strain amplitude of 1% has been constructed by vertically shifting the curves at other strain amplitudes for various aging temperatures: **a** 80 °C, **b** 100 °C and **c** 120 °C.

strain amplitude-dependent storage modulus of Fig. 2, which indicates that the storage modulus decreases with increasing dynamic strain amplitude.

The hysteresis loss plays an important role in the tearing energy and fatigue crack growth rate of the rubber-like materials[35]. To quantify the energy dissipation, the integrated area of the hysteresis loop was calculated, as shown in Fig. 6. The results depict that the hysteresis loss increases with the aging time and dynamic strain amplitude for each aging temperature. Generally, the hysteresis is caused by friction between the rubber matrix and filler particles[36]. In addition, with increasing of aging time, more ruptured chains and low-molecular-weight products are generated[37], which results in obvious hysteresis responses. It can be seen that the hysteresis loss of the specimen aged at 120 °C is more remarkable, which may be related to stronger internal friction and impact between CB fillers and the molecular chains.

It is apparent that the hysteresis loss curves at various dynamic strain amplitudes are parallel to each other. It is well known that the experimental curves of rubber-like materials can usually be shifted horizontally or vertically to accelerate the prediction of the mechanical properties. On the basis of this method, a master curve at a reference dynamic strain amplitude of 1% has been constructed by vertically shifting the curves at other strain amplitudes, and the results are shown in Fig. 7. The corresponding vertical shift factors of the hysteresis loss are shown in Fig. 8, and the results reflect that the vertical shift factors are proportional to the dynamic strain amplitudes. More interestingly, for the same strain amplitude, the vertical shift factors at the different aging temperatures are identical, which indicates that the vertical shift factors are irrelevant to the aging temperature. Thus, if the vertical shift factors can be determined, the hysteresis loss versus aging time of the material at arbitrary dynamic strain amplitude can be

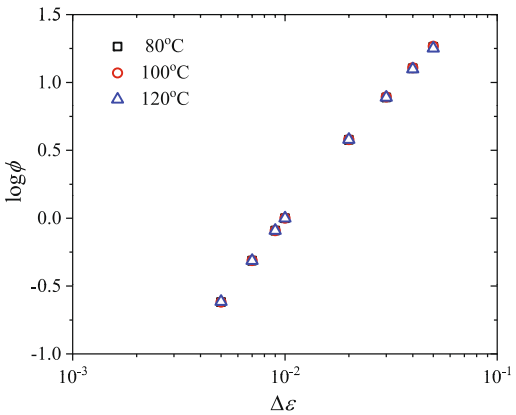

Fig. 8 Vertical shift factors versus dynamic strain amplitude. The vertical shift factors are proportional to the dynamic strain amplitudes, and for the same strain amplitude, the vertical shift factors for different aging temperatures are identical.

obtained as the following equation:

$$D(t, \Delta\varepsilon) = \phi D(t, \Delta\varepsilon_0) \tag{12}$$

where D is the hysteresis loss, t is the aging time, $\Delta\varepsilon$ is the dynamic strain amplitude, $\Delta\varepsilon_0$ is the reference dynamic strain amplitude, and ϕ is the shift factor.

As mentioned above, the hysteresis loss for all cases indicated in Fig. 6 can be predicted by taking Eq. (11) into Eq. (8), which shows that the hysteresis loss can be constructed as a function of aging time and dynamic strain amplitude. It should be noted that E''_m is a function of aging time, and the corresponding expressions of different aging temperatures are shown in Fig. 4. The theoretical prediction results are shown in Fig. 9 along with the

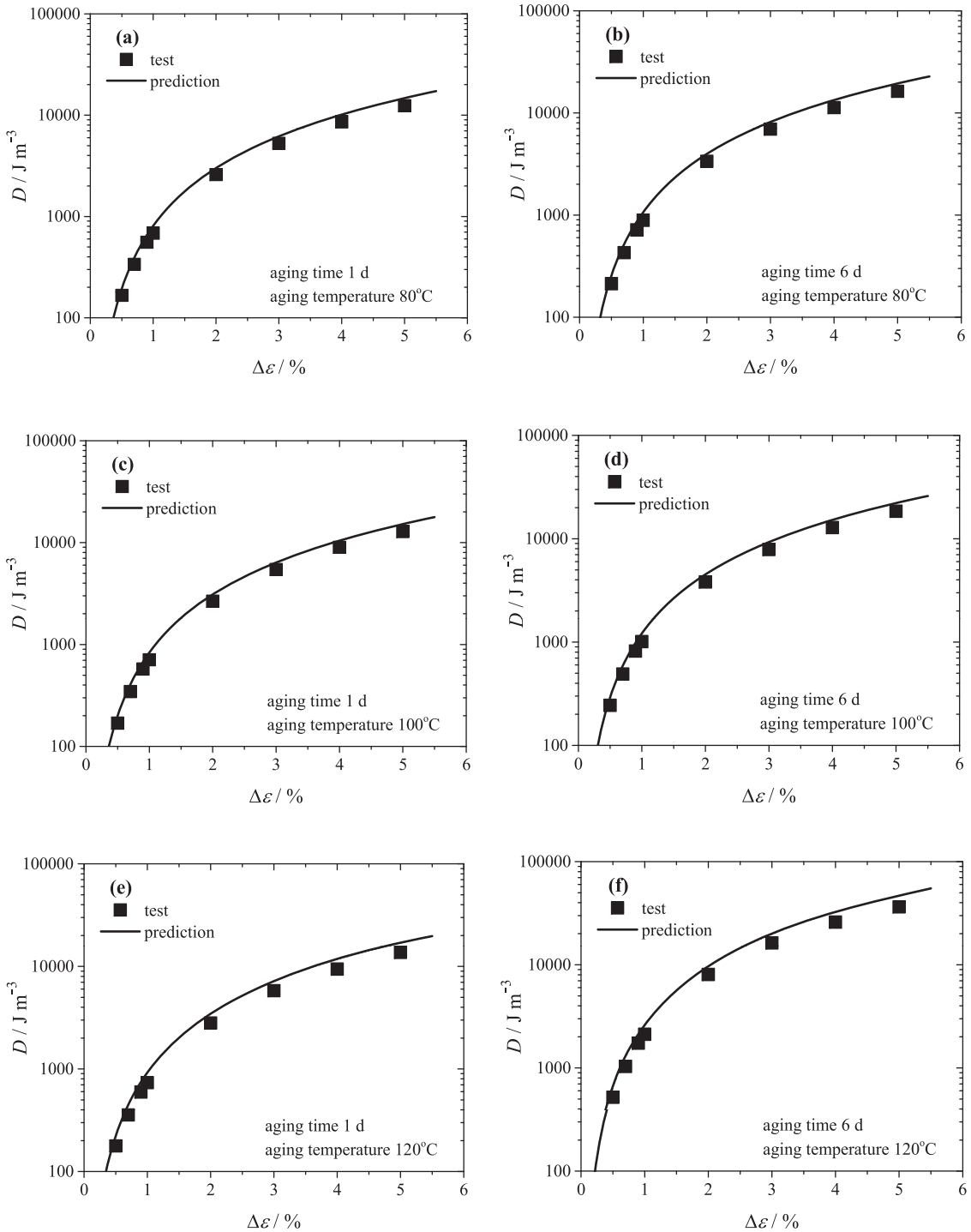

Fig. 9 Hysteresis loss prediction results vs. experiments. Scatters are the experimental results, and solid lines are the model prediction results. **a**, **b** The results for aging temperature 80 °C, **c**, **d** the results for aging temperature 100 °C, **e**, **f** the results for aging temperature 120 °C.

test results. It is obvious that the model prediction results are in good agreement with the experiments. It means that, once the Payne effect is known, the hysteresis loss for a given applied strain amplitude at arbitrary aging conditions can be predicted.

To summarize, the effects of thermo-oxidative aging on the Payne effect and hysteresis loss of CB filled natural rubber vulcanizates were investigated. In the dynamic strain amplitude sweep tests, it can be observed that both the storage modulus and the loss modulus increase with increasing aging time and aging temperature. The Payne effect becomes increasingly obvious with increasing aging time for higher aging temperatures. The hysteresis loss increases with the aging time and dynamic strain amplitude for the aging temperatures. It is apparent that the hysteresis loss curves at various dynamic strain amplitudes are parallel to each other, and a master curve can be constructed at a reference dynamic strain amplitude by vertically shifting curves for other strain amplitudes. The corresponding vertical shift factors of the hysteresis loss are proportional to the dynamic strain amplitudes. Based on this relationship, an accelerated method to predict the hysteresis

Fig. 10 The specimens in the aging oven. Vulcanizate strips are hung dispersedly in the temperature-controlled air-aging oven to ensure uniformly aging.

loss versus aging time of the material at arbitrary dynamic strain amplitude has been proposed. The Kraus model is used to describe the Payne effect and a viscoelastic model consisting of dynamic strain amplitude and loss modulus is used to calculate the energy dissipation. The model predictions are in good agreement with the experimental results.

METHODS

Materials

The material used for mechanical testing in this work is CB filled natural rubber vulcanizate with a Shore-A hardness of 69, which is provided by Zhuzhou Times New Material Technology Co., Ltd. China. The main formulation is as follows: 100 phr natural rubber (Thailand RRS3), 56 phr carbon black (N330), 2.2 phr sulfur, 2 phr antioxidant, 5 phr zinc oxide, 0.8 phr vulcanization accelerator, and 2 phr stearic acid.

Thermal-oxidative aging

In the scope of this research work, thermo-oxidative aged vulcanizates were subjected to dynamic mechanical excitations. Thermo-oxidative aging of vulcanizate strips was carried out in a temperature-controlled air-aging oven. To keep the specimen's surface temperature isothermal, the specimens were hung in the aging oven, as shown in Fig. 10. The previous work by Li[8] demonstrated that the change of mechanical properties, such as elastic modulus, tensile strength, tear strength, etc., of the aged CB filled natural rubber vulcanizates depend on the aging temperature, and the higher the aging temperature, the more pronounced change in mechanical properties. To investigate the influences of aging temperature and aging time on the Payne effect and the hysteresis loss of the CB filled rubber vulcanizates, the selected aging temperatures for the specimens in this work were 80, 100 and 120 °C, and the aging time ranged from 1 day to 6 days.

Dynamic mechanical analysis (DMA)

In this paper, the specimens with dimensions of $25 \times 5 \times 2\ mm^3$ for DMA tests were cut from the thermo-oxidative aged vulcanizate strips, and all tests were carried out with a Gabo Eplexor 500 N test machine working in the tensile mode. First, the specimens were preconditioned with a cyclic strain-controlled process to exclude the Mullins effect. The Mullins effect corresponds to a softening phenomenon during the first few cycles. The first 6 cycles were chosen to exclude the Mullins effect, and the dynamic strain amplitude was 15% during these cycles, which was not less than the maximum dynamic strain amplitude in the subsequent Payne effect investigation. Afterward, the specimens were sinusoidally stretched at a constant temperature of 23 °C and a fixed frequency of 10 Hz. The prestrain was 10%, and the dynamic strain amplitudes ranged from 0.1% to 5% in steps of 0.1%. The storage modulus, loss modulus and hysteresis loop versus dynamic strain amplitude under various thermo-oxidative aging times were recorded.

DATA AVAILABILITY

The data used that support the findings of this study are available upon request to Boyuan Yin (Yinboyuanxtu@163.com).

Received: 5 July 2022; Accepted: 2 November 2022;
Published online: 14 November 2022

REFERENCES

1. Rabanizada, N., Lupberger, F., Johlitz, M. & Lion, A. Experimental investigation of the dynamic mechanical behaviour of chemically aged elastomers. *Arch. Appl. Mech.* **85**, 1011–1023 (2015).
2. Sharma, H. N. et al. Moisture outgassing from siloxane elastomers containing surface-treated-silica fillers. *npj Mat. Degrad.* **3**, 1–9 (2019).
3. Jebur, Q. H., Jweeg, M. J., Al-Waily, M., Ahmad, H. Y. & Resan, K. K. Hyperelastic models for the description and simulation of rubber subjected to large tensile loading. *Sci. Eng.* **108**, 75–85 (2021).
4. Hu, X. L., He, R. Z., Huang, Y. J., Yin, B. Y. & Luo, W. B. A method to predict the dynamical behaviors of carbon black filled natural rubber at different temperatures. *Polym. Test.* **79**, 106067 (2019).
5. Yao, B. B., Xia, L. J., Wang, H. & Kan, Z. The effects of natural astaxanthin-modified silica on properties of natural rubber. *J. Appl. Polym. Sci.* **136**, 47287 (2019).
6. Araki, O., Shimamoto, T. & Masuda, T. Physical aging of polystyrene investigated by dynamic viscoelasticity. *J. Polym. Sci. Pol. Phys.* **42**, 4433–4437 (2015).
7. Lacount, B. J., Castro, J. M. & Ignatz-Hoover, F. Development of a service-simulating, accelerated aging test method for exterior tire rubber compounds II. Design and development of an accelerated outdoor aging simulator. *Polym. Degrad. Stabil.* **75**, 213–227 (2002).
8. Li, Y., Liu, X., Hu, X. L. & Luo, W. B. Changes in tensile and tearing fracture properties of carbon-black filled rubber vulcanizates by thermal aging. *Polym. Advan. Technol.* **26**, 1331–1335 (2015).
9. Dinari, A., Zaïri, F., Chaabane, M., Ismail, J. & Benameur, T. Thermo-oxidative stress relaxation in carbon-filled SBR. *Plast. Rubber Compos.* **50**, 425–440 (2021).
10. Aziz, S. A. A. et al. Thermal aging rheological behavior of magnetorheological elastomers based on silicone rubber. *Int. J. Mol. Sci.* **21**, 9007 (2020).
11. Hou, F. Y., Song, Y. H. & Zheng, Q. Payne effect of thermo-oxidatively aged isoprene rubber vulcanizates. *Polymer* **195**, 122432 (2020).
12. Shi, X. Y. et al. Influence of carbon black on the payne effect of filled natural rubber compounds. *Compos. Sci. Technol.* **203**, 108586 (2021).
13. Ouyang, G. B. Modulus, hysteresis and the Payne effect. *Kautsch. Gummi Kunstst.* **59**, 332–343 (2006).
14. Jiang, B. W., Zhu, L. Q., Zhao, C. Z. & Chen, Z. R. An investigation on the bound rubber and dynamic mechanical properties of polystyrene particles-filled elastomer. *Polym. Composite.* **38**, 1112–1117 (2015).
15. Ma, J. H., Zhang, L. Q. & Wu, Y. P. Characterization of filler-rubber interaction, filler network structure, and their effects on viscoelasticity for styrene-butadiene rubber filled with different fillers. *J. Macromol. Sci. Part B* **52**, 1128–1141 (2013).
16. Ning, N. Y. et al. A quantitative approach to study the interface of carbon nanotubes/elastomer nanocomposites. *Eur. Polym. J.* **102**, 10–18 (2018).
17. Fu, W. & Wang, L. Variation of the Payne effect in natural rubber reinforced by graft-modified carbon black. *J. Macromol. Sci. Part B* **56**, 53–63 (2017).
18. Kraus, G. Swelling of filler-reinforced vulcanizates. *J. Appl. Polym. Sci.* **7**, 861–871 (1963).
19. Pan, Y. & Zhong, Z. A viscoelastic constitutive modeling of rubber-like materials with the Payne effect. *Appl. Math. Model.* **50**, 621–632 (2017).
20. Ahose K. D., Lejeunes, S., Eyheramendy, D. & Bouaziz, R. Modeling and numerical simulation of thermal ageing in a filled rubber. In Constitutive Models for Rubber XI. 535–541 (CRC Press, 2019).
21. Wei, Y. T., Nasdala, L., Rothert, H. & Xie, Z. Experimental investigations on the dynamic mechanical properties of aged rubbers. *Polym. Test.* **23**, 447–453 (2004).
22. Du, Y. Q., Zheng, J. & Yu, G. Influence of thermally-accelerated aging on the dynamic mechanical properties of HTPB coating and crosslinking density-modified model for the Payne effect. *Polymers* **12**, 403 (2020).
23. Alam, M., Mandal, S. K., Roy, K. & Debnath, S. K. Synergism of novel thiuram disulfide and dibenzothiazyl disulfide in the vulcanization of natural rubber:

curing, mechanical and aging resistance properties. *Int. J. Ind. Chem.* **5**, 1–11 (2014).
24. Rizwan, M. & Chandan, M. R. Mechanistic insights into the ageing of EPDM micro/hybrid composites for high voltage insulation application. *Polym. Degrad. Stabil.* **204**, 110114 (2022).
25. Kadri, R., Abdelaziz, M. N., Fayolle, B., Hassine, M. B. & Witz, J. F. A unified mechanical based approach to fracture properties estimates of rubbers subjected to aging. *Int. J. Solids Struct.* **234**, 111305 (2022).
26. Wang, M. Y. et al. Effect of non-rubber components on the crosslinking structure and thermo-oxidative degradation of natural rubber. *Polym. Degrad. Stabil.* **196**, 109845 (2022).
27. Wang, X. L., Yang, K. & Zhang, P. Evaluation of the aging coefficient and the aging lifetime of carbon black-filled styrene-isoprene-butadiene rubber after thermal-oxidative aging. *Compos. Sci. Technol.* **220**, 109258 (2022).
28. Kucherskii, A. M. Hysteresis losses in carbon-black-filled rubbers under small and large elongations. *Polym. Test.* **24**, 733–738 (2005).
29. Luo, W. B., Hu, X. L., Wang, C. H. & Li, Q. H. Frequency- and strain-amplitude-dependent dynamical mechanical properties and hysteresis loss of CB-filled vulcanized natural rubber. *Int. J. Mech. Sci.* **52**, 168–174 (2010).
30. Pistor, V., Ornaghi, F. G., Ornaghi, H. L. & Zattera, A. J. Dynamic mechanical characterization of epoxy/epoxycyclohexyl–POSS nanocomposites. *Mater. Sci. Eng. A* **532**, 339–345 (2012).
31. Qazvini, N. T. & Mohammadi, N. Dynamic mechanical analysis of segmental relaxation in unsaturated polyester resin networks: effect of styrene content. *Polymer* **46**, 9088–9096 (2005).
32. Yin, B. Y., Hu, X. L., Luo, W. B. & Song, K. Application of fractional calculus methods to asymmetric dynamical response of CB-Filled rubber. *Polym. Test.* **61**, 416–420 (2017).
33. Jawaid, M., Khalil, H. P. S. A., Hassan, A., Dungani, R. & Hadiyane, A. Effect of jute fibre loading on tensile and dynamic mechanical properties of oil palm epoxy composites. *Compos. Part B-Eng.* **45**, 619–624 (2013).
34. Cho, J. H. & Youn, S. K. A viscoelastic constitutive model of rubber under small oscillatory load superimposed on large static deformation considering the Payne effect. *Arch. Appl. Mech.* **75**, 275–288 (2006).
35. Hassim, D. H. A. I., Abraham, F., Summerscales, J. & Brown, P. Fatigue crack growth of natural rubber/butadiene rubber blend containing waste tyre rubber powders. *Solid State Phenom.* **317**, 293–299 (2021).
36. Aini, N. A. M., Othman, N., Hussin, M. H., Sahakaro, K. & Hayeemasae, N. Hydroxymethylation-modified lignin and its effectiveness as a filler in rubber composites. *Processes* **7**, 315 (2019).
37. Zhang, J. H. et al. Thermal-oxidative aging behaviors of shape memory nitrile butadiene rubber composite with dual crosslinking networks. *Polym. Degrad. Stabil.* **179**, 109280 (2020).

ACKNOWLEDGEMENTS

This work was supported by the National Natural Science Foundation of China (12072308), the Natural Science Foundation of Hunan Province (2021JJ30644), the Scientific Research Foundation of Hunan Province Education Department (20C0796) and the Youth Foundation of Hunan University of Science and Technology.

AUTHOR CONTRIBUTIONS

B.Y.Y. contributed to the conception, the DMA tests and the original draft writing. H.B.W. contributed to the sample preparation and the experimental data processing. W.B.L. contributed to the methodology and manuscript revision. W.B.L. and B.Y.Y. acquired the fundings.

COMPETING INTERESTS

The authors declare no competing interests.

ADDITIONAL INFORMATION

Correspondence and requests for materials should be addressed to Wenbo Luo.

Reprints and permission information is available at http://www.nature.com/reprints

Publisher's note Springer Nature remains neutral with regard to jurisdictional claims in published maps and institutional affiliations.